ARTICLE
Journal of Cellular Biochemistry 116:2882–2895 (2015)

Journal of Cellular Biochemistry

An Involvement of PI3-K/Akt Activation and Inhibition of AIF Translocation in Neuroprotective Effects of Undecylenic Acid (UDA) Against Pro-Apoptotic Factors-Induced Cell Death in Human Neuroblastoma SH-SY5Y Cells

Danuta Jantas,[1]* Marek Piotrowski,[2] and Wladyslaw Lason[1]

[1]*Department of Experimental Neuroendocrinology, Institute of Pharmacology, Polish Academy of Sciences, Krakow, Poland*

[2]*Jerzy Haber Institute of Catalysis and Surface Chemistry, Polish Academy of Sciences, Krakow, Poland*

ABSTRACT

Undecylenic acid (UDA), a naturally occurring 11-carbon unsaturated fatty acid, has been used for several years as an economical antifungal agent and a nutritional supplement. Recently, the potential usefulness of UDA as a neuroprotective drug has been suggested based on the ability of this agent to inhibit μ-calpain activity. In order to verify neuroprotective potential of UDA, we tested protective efficacy of this compound against cell damage evoked by pro-apoptotic factors (staurosporine and doxorubicin) and oxidative stress (hydrogen peroxide) in human neuroblastoma SH-SY5Y cells. We showed that UDA partially protected SH-SY5Y cells against the staurosporine- and doxorubicin-evoked cell death; however, this effect was not connected with its influence on caspase-3 activity. UDA decreased the St-induced changes in mitochondrial and cytosolic AIF level, whereas in Dox-model it affected only the cytosolic AIF content. Moreover, UDA (1–40 μM) decreased the hydrogen peroxide-induced cell damage which was connected with attenuation of hydrogen peroxide-mediated necrotic (PI staining, ADP/ATP ratio) and apoptotic (mitochondrial membrane potential, caspase-3 activation, AIF translocation) changes. Finally, we demonstrated that an inhibitor of PI3-K/Akt (LY294002) but not MAPK/ERK1/2 (U0126) pathway blocked the protection mediated by UDA in all tested models of SH-SY5Y cell injury. These in vitro data point to UDA as potentially effective neuroprotectant the utility of which should be further validated in animal studies. J. Cell. Biochem. 116: 2882–2895, 2015.

KEY WORDS: STAUROSPORINE; DOXORUBICIN; HYDROGEN PEROXIDE; CALPAIN INHIBITOR; NEUROPROTECTION; APOPTOSIS

Undecylenic acid (UDA, 10-undecenoic acid, $C_{11}H_{20}O_2$) is an 11-carbon monounsaturated fatty acid (MUFA) which is commercially used as an economical natural compound which possesses antifungal, antibacterial, and antiviral properties [Monograph, 2002]. It is produced by the vacuum distillation of castor bean oil, via the pyrolysis of ricinoleic acid and has been used for several years as the active ingredient in many topical over-the-counter antifungal preparations and a nutritional supplement for maintaining a healthy balance of intestinal and vaginal microbial flora [Monograph, 2002; Van der Steen and Stevens, 2009]. On the basis of observations of a continued marketing of UDA in the USA as a nutritional supplement over many years, UDA is thought to be a quite safe drug in humans [Monograph, 2002; Brayden and Walsh, 2014]. Since UDA is a water insoluble

Abbreviations: AIF, apoptosis inducing factor; DHA, docosahexaenoic acid; Dox, doxorubicin; EPA, eicosapentaenoic acid; FBS, fetal bovine serum; H_2O_2, hydrogen peroxide; LDH, lactate dehydrogenase; MAPK/ERK1/2, mitogen-activated protein kinase/extracellular signal-regulated kinase 1/2; MUFA, monounsaturated fatty acid; MTT, 3-(4,5-dimethylthiazol-2-yl)-2,5-diphenyltetrazolium bromide; PI, propidium iodide; PI3-K/Akt, Phosphatidylinositol-3 kinase/Protein kinase Akt; PUFA, polyunsaturated fatty acid; ROS, reactive oxygen species; St, staurosporine; UDA, undecylenic acid (10-undecenoic acid).

Conflicts of interest: None

Grant sponsor: Institute of Pharmacology, Polish Academy of Sciences; Grant sponsor: National Centre for Research and Development; Grant number: Pol-Nor/199523/64/2013.

*Correspondence to: Danuta Jantas, Ph.D., Department of Experimental Neuroendocrinology, Institute of Pharmacology, Polish Academy of Sciences, Smetna 12, PL 31-343 Krakow, Poland.
E-mail: jantas@if-pan.krakow.pl

Manuscript Received: 27 March 2015; Manuscript Accepted: 15 May 2015

Accepted manuscript online in Wiley Online Library (wileyonlinelibrary.com): 27 May 2015

DOI 10.1002/jcb.25236 • © 2015 Wiley Periodicals, Inc.

compound, its vinyl ester derivatives have been synthesized to enhance its water solubility. These modifications improved the UDA surface tension activity and biodegradability, enabling its antimicrobial use in food, cosmetics, and medicine [Raku et al., 2003; Tokiwa et al., 2007]. Recently, an additional clinical use of UDA has been proposed as a promising component of formulations for parenteral drug and peptide delivery (e.g., insulin, rapamycin) [Kovalainen et al., 2013; Brayden and Walsh, 2014; Shrestha et al., 2014; Nieto et al., 2015]. Recent data from nanopharmacology demonstrated that UDA could be an important component of nanoformulations for augmented cellular trafficking and endosome escape of some anticancer drugs [Tabasi et al., 2012; Almeida et al., 2014; Shahbazi et al., 2014]. Interestingly, UDA was naturally found in the body excretion fluids (e.g., in sweat) and can be a component of cell membrane phospholipids as shown in the study on rat synaptosomes [Wei et al., 1987; Monograph, 2002]. Other recently proposed biological functions for UDA include (i) anti-aging properties connected with its stimulatory effect on human type I collagen synthesis [Hashem et al., 2008]; (ii) induction of osteoblast differentiation through the upregulation of transcription factors, AP-1 and NFATc1 [Kim et al., 2010]; and (iii) neuroprotective potential assumed on the basis of ability of UDA to inhibit μ-calpain (a calcium-activated cysteine protease) activity in a high throughput screening assay using fluorescent probe [Kang et al., 2009]. The latter feature of UDA was confirmed in SH-SY5Y and HEK293T cells with overexpression of the catalytic subunit of μ-calpain where UDA reduced μ-calpain activity with better potency than the classic calpain inhibitor, MDL28170 [Lee et al., 2012]. Therefore, UDA has been suggested to be a novel non-peptide-like μ-calpain inhibitor with good cell permeability and putative neuroprotective effect which was demonstrated in models of SH-SY5Y cell injury evoked by amyloid β (Aβ), glutamate, and hydrogen peroxide (H_2O_2) [Lee et al., 2012], although it was tested only in one concentration (20 μM). Of possible neuroprotective mechanisms responsible for UDA-mediated neuroprotection, an inhibition of Aβ oligomerization and fibrillation, scavenging reactive oxygen species (ROS), downregulation of pro-apoptotic proteins (caspase-3, PARP, p25), and inhibition of μ-calpain activity have been proposed [Lee et al., 2012].

In order to better understand the protective potential of UDA and intracellular mechanisms involved in its action, we tested a wide concentration range of that compound (0.01–40 μM) in human neuroblastoma SH-SY5Y cells against cell death induced by agents activating intracellular (staurosporine, St) and extracellular (doxorubicin, Dox) apoptotic pathway, and by elevated oxidative stress (H_2O_2). Apart from showing a general neuroprotective profile of UDA in cell toxicity/viability assays, we employed additional markers, like reactive oxygen species (ROS) generation, ADP/ATP ratio measurement, calpain and caspase-3 activity, Western blot analysis of apoptosis inducing factor (AIF) in mitochondrial and cytosolic cell fractions. Moreover, we verified the participation of pro-survival intracellular pathways, PI3-K/Akt and MAPK/ERK1/2 [Hetman and Gozdz, 2004; Burke, 2007; Ahn, 2014], in neuroprotective action of UDA by using their specific inhibitors, LY294002 and U0126, respectively.

MATERIALS AND METHODS

REAGENTS

Dulbecco's modified Eagle medium (DMEM), fetal bovine serum (FBS), and FluoroBrite™ DMEM were from Gibco (Invitrogen, Poisley, UK). The Cytotoxicity Detection Kit and BM Chemiluminescence Western Blotting Kit were from Roche Diagnostic (Mannheim, Germany). EnzyLight™ ADP/ATP Ratio Assay Kit (ELD-100) was from BioAssay Systems (CA). 5-(and-6)-chloromethyl-2′,7′-dichlorodihydrofluorescein diacetate, acetyl ester (CM-H_2DCFDA, cat. No C6827) was from Molecular Probes (OR). Primary polyclonal rabbit antibodies: anti-spectrin α II (sc-48382), anti-β-actin (sc-47778), anti-AIF (sc-5586) and anti-GAPDH (sc-25778), MW standards (sc-2035), and goat anti-rabbit secondary antibodies (sc-2004 and sc-2030) were purchased from Santa Cruz Biotechnology, Inc. (CA). Hydrogen peroxide (30% solution) was from POCH (Gliwice, Poland). All other reagents were from Sigma (Sigma–Aldrich Chemie GmbH, Germany).

CELL CULTURE

Human neuroblastoma SH-SY5Y cells (ATCC, passages 5–20) were grown in DMEM supplemented with a 10% heat-inactivated FBS and 1% penicillin/streptomycin mixture. Cells were maintained at 37°C in a saturated humidity atmosphere containing 95% air and 5% CO_2. The cells, after having reached 80% confluence, were trypsynized and seeded at a density of 6×10^5 cells per ml into multi-well plates. Cells were counted using LUNA™ Automatic Cell Counter (Logos Biosystems, Inc., Korea). One day before cell treatment, the culture medium was replaced by DMEM containing antibiotics and 1% FBS.

CELL TREATMENT

In the model of St- and Dox-evoked cell damage, the SH-SY5Y cells were treated with vehicle (0.1% DMSO), toxin alone (St 0.15 μM or Dox 0.25 μM), toxin+ UDA (0.1–20 μM), and toxin + Ac-DEVD-CHO (10 μM, caspase-3 inhibitor) for 24 h. In the model of oxidative stress (H_2O_2)-evoked cell death, the cells were treated with vehicle (0.1% DMSO), UDA alone (10 and 20 μM), H_2O_2 alone (1 and 0.5 mM for 6 and 24 h, respectively), H_2O_2 + UDA (0.1–40 μM), and H_2O_2 + MDL28170 (10 μM, calpain inhibitor) for 6 and 24 h. The effective concentrations of St, Dox, and H_2O_2 were established in our previous study where those factors evoked about 50% reduction in SH-SY5Y cell viability (MTT reduction assay) [Jantas et al., 2008; Piotrowski et al., 2013]. The chosen end points of cell treatment for other measurements (caspase-3 activity, calpain activity, ROS production, $\Delta\Psi$m, ADP/ATP ratio; AIF level) were adjusted on the basis of previous our and others' data [Jantas et al., 2008,2009, 2011, 2015; Son et al., 2009; Richter et al., 2015]. In order to elucidate the involvement of pro-survival intracellular pathways in neuroprotection mediated by UDA, the cell treatment with protective and cell-damaging agents was preceded by 30 min pretreatment with LY294002 (10 μM) and U0126 (10 μM), an inhibitors of PI3-K/Akt and MAPK/ERK1/2 pathways, respectively.

Dox and N-acetylcysteine (NAC) were dissolved in distilled water and stored at −20°C. UDA (10 mM), MDL18270 (10 mM), Ac-DEVD-CHO (10 mM), LY294002 (10 mM), U0126 (10 mM), and St (100 mM)

stock solutions were prepared in DMSO and stored at −20°C. Dilutions of the tested chemicals were prepared in distilled water and were added to the culture medium at indicated concentrations under light limited conditions. Each experimental set of the control cultures was supplemented with the same amount of the appropriate vehicle and the solvent was present in cultures at a final concentration of 0.1%.

CELL VIABILITY ASSAY

The cell viability assessment was done 6 (for 1 mM H_2O_2) and 24 h (for 0.5 mM H_2O_2, St, and Dox) after treatment of cells with the agents. The cell damage was quantified using a tetrazolium salt colorimetric assay with 3-[4,5-dimethylthylthiazol-2-yl]-2,5-diphenyltetrazolium bromide (MTT) as described previously [Jantas et al., 2008]. The absorbance of each sample was measured at 570 nm using a 96-well plate-reader (Infinite® M200 PRO, Tecan, Switzerland). The data were normalized to the absorbance in the vehicle-treated cells (100%) and expressed as a percent of the control ± SEM established from three independent experiments with five replicates.

ASSESSMENT OF CELL INTEGRITY: LDH RELEASE ASSAY AND PI STAINING

In order to estimate cell death, the level of lactate dehydrogenase (LDH) released from damaged cells into culture media was measured after 24 h of treatment of SH-SY5Y with UDA (0.1–40 μM), MDL18270 (10 μM), and H_2O_2 (0.5 mM) according to the method described previously [Jantas et al., 2008]. The intensity of red color formed in the assay (Cytotoxicity Detection Kit, Roche) was measured at a wavelength of 490 nm and absorbance of blanks, determined as no-enzyme control, has been subtracted from each value. The data were normalized to the total LDH release (Triton X-100-treated cells, 100%) and are presented as the mean ± SEM from three independent experiments with five replicates.

For confirmation of the data obtained by biochemical LDH release assay, we stained the cells with the propidium iodide (PI) which diffuses into cells once the plasma membrane becomes permeabilized. The cells were stained with PI and analyzed by flow cytometry as described previously [Jantas et al., 2015]. 1×10^4 cells were analyzed using BD FACSCanto II System and BD FACSDiva™ v5.0.1 Software (BD Biosciences). Data were shown as a percentage of PI-positive cells (mean ± SEM) from three independent experiments with three replicates.

MEASUREMENT OF INTRACELLULAR REACTIVE OXYGEN SPECIES FORMATION

Free radical production was measured by incubating the cells with the fluorescent probe 5-(and-6)-chloromethyl-2′,7′-dichlorodihydrofluorescein diacetate, acetyl ester (CM-H_2DCFDA, Molecular Probe, USA) according to manufacturer's protocol. Non-fluorescent CM-H_2DCFDA crosses easily cell membranes and after removal of acetyl group by esterase, it becomes the fluorescent product CM-DCF, the fluorescence of which increases after oxidation (with peroxide and superoxide). CM-DFC is regarded to possesses improved retention and photostability in cells when compared to the chemically non-modified probe, DCF [Halliwell and Whiteman, 2004; Rhee et al., 2010]. To assess intracellular ROS generation in the model of H_2O_2-evoked cell damage, we used a modified method as described previously [Taki-Nakano et al., 2014] where the cells were first loaded with 5 μM CM-H_2DCFDA in FluoroBrite™ DMEM and placed in an incubator for 30 min. After washing twice with pre-warmed FluoroBrite™ DMEM, the cells were treated with UDA (0.1–40 μM), MDL28170 (10 μM), NAC (0.5 mM), and H_2O_2 (0.5 mM) for the next 60 min. After the next washing, the fluorescence was measured using excitation and emission wavelengths of 485 nm and 535 nm, respectively, in a microplate fluorescence reader (Infinite® M200 PRO, Tecan, Switzerland).

In the models of St- and Dox-evoked cell damage in SH-SY5Y cells, we used a method described previously [Jantas et al., 2009; Yamada et al., 2011] where first the cells were treated with drugs and later loaded with the fluorescent probe to measure ROS level. Briefly, the SH-SY5Y cells were treated for 3–9 h with St (0.15 μM) or Dox (0.25 μM) in order to find an endpoint where intracellular ROS significantly increased to measure the impact of neuroprotectants. After cell treatment, the cells were washed once with pre-warmed FluoroBrite™ DMEM and loaded with 5 μM CM-H_2DCFDA in FluoroBrite™ DMEM for 30 min. After two washings, the fluorescence was measured, the data were normalized to vehicle-treated cells (100%) and presented as the mean ± SEM from three independent experiments with five replicates. Antioxidant, N-acetylcysteine (0.5 mM) was used as a positive control for the assay. Representative microphotographs of cells loaded with CM-H_2DCFDA and treated for 1 h with UDA (10 and 40 μM), NAC (0.5 mM) and H_2O_2 (0.5 mM) were taken with the inverted fluorescence microscope (AxioObserver, Carl Zeiss) using differential interference contrast (DIC) and fluorescence (excitation with 470 nm) live imaging methods.

ASSESSMENT OF CASPASE-3 ACTIVITY

Caspase-3 activity was measured by biochemical method employing the fluorogenic substrate, Ac-DEVD-AMC as described in detail previously [Jantas et al., 2015]. The SH-SY5Y cells were seeded at the density of 1.5×10^6 cells/well and treated with UDA (1–20 μM), caspase-3 inhibitor (Ac-DEVD-CHO, 10 μM), calpain inhibitor (MDL28170, 10 μM) and H_2O_2 (0.5 mM), St (0.15 μM), or Dox (0.25 μM) for 9 h. The fluorescence of each experimental group was measured with a microplate fluorescence reader (Infinite® M200 PRO, Tecan, Switzerland) at 360 and 460 nm excitation and emission wavelengths, respectively. The caspase-3 activity was calculated per mg protein. The protein concentration in cell lysates was determined with the bicinchoninic acid protein assay kit (BCA1, Sigma). The data were normalized to the vehicle-treated cells (100%) and expressed as the mean ± SEM from three independent experiments with two replicates.

MEASUREMENT OF CHANGES IN MITOCHONDRIAL MEMBRANE POTENTIAL (ΔΨM)

The ΔΨm was assessed using the fluorescent probe tetramethylrhodamine ethyl ester (TMRE) according to the method described by Yin et al. [2011]. Briefly, the cells after treatment with UDA (0.1–40 μM), MDL28170 (10 μM) and H_2O_2 (0.5 mM for 6 h), St (0.15 μM for 9 h), or Dox (0.25 μM for 9 h) were loaded with 100 nM TMRE in

FluoroBrite™ DMEM and placed in an incubator for 20 min. After two washings with pre-warmed FluoroBrite™ DMEM, the fluorescence was measured in a microplate fluorescence reader (Infinite® M200 PRO, Tecan, Switzerland) with excitation and emission wavelengths of 540 and 595 nm, respectively. Valinomycin (val, 10 μM for 5 min), a K^+-selective ionophore and mitochondria depolarizating agent, was used as a positive control for the assay [Lofrumento et al., 2011]. Data after subtraction of blanks (fluorescence of cells without TMRE) were normalized to vehicle-treated cells (100%) are presented as the mean ± SEM from three independent experiments with five replicates.

ADP/ATP ASSAY

Changes in ADP/ATP after 18 h of treatment of SH-SY5Y cells with UDA (1 and 10 μM) and H_2O_2 (0.5 mM) were measured by EnzyLight™ ADP/ATP Ratio Assay Kit (ELD-100) strictly according to the manufacturer's protocol (BioAssay Systems). Luminescence was measured in a microplate luminescence reader (MicroBeta TriLux 1450LSC8 Luminescence Counter, Perkin Elmer). The calculated ADP/ATP ratio is shown as the mean ± SEM from two independent experiments with three replicates.

PROTEIN EXTRACTS AND IMMUNOBLOTS

The SH-SY5Y cells seeded in 6-well plates at the density of 1.5×10^6 cells/well were treated for 9 h with UDA (1–20 μM) and H_2O_2 (0.5 mM) for spectrin α II products measurement. For mitochondrial and cytosolic apoptosis inducing factor (AIF) measurement, the cells were treated for 14 h with UDA (1–20 μM) and H_2O_2 (0.5 mM) and St (0.15 μM) or for 18 h with UDA (1–10 μM) and Dox (0.25 μM). The whole cell lysates (for spectrin α II) and cytosolic and mitochondrial cellular fractions were prepared as described in detail previously [Jantas et al., 2011, 2015]. An equal amount of protein from experimental groups was separated on a 7% (for spectrin α II) or 10% (for AIF) SDS–polyacrylamide gels and transferred onto a PVDF membrane. Membranes after blocking with 5% nonfat milk were incubated overnight with primary antibodies diluted at 1:500 (spectrin α II, AIF, GAPDH) and 1:2,000 (β-actin) in 1% nonfat milk. The amount of β-actin and GAPDH was determined on the same membrane on which the spectrin α II and AIF were measured by stripping and reprobing the membrane as described previously [Jantas et al., 2011]. Immunocomplexes were detected using an enhanced chemiluminescence detection system (BM Chemiluminescence Western Blotting Kit, Roche) and band intensities were determined by densitometric analysis of immunoblots (Fuji Film Las 4000). MultiGauge v.3 Software was used for quantification of Western blot signals. Data from duplicate determinations in three independent experiments were normalized to β-actin and GAPDH level for spectrin α II and AIF, respectively.

DATA ANALYSIS

Data after normalization were expressed as the mean ± SEM and analyzed using the Statistica software (StatSoft, Inc., Tulsa, OK). The analysis of variance (one-way ANOVA) and posthoc Tukey's test for multiple comparisons were used to assess statistical significance at $P < 0.05$.

RESULTS

UDA ATTENUATES THE STAUROSPORINE (ST)- AND DOXORUBICIN (DOX)-INDUCED CELL DAMAGE

In order to study the effect of UDA on apoptotic processes, we used St and Dox as pro-apoptotic factors inducing mainly intracellular (mitochondrial) and extracellular (via death receptor) apoptotic pathway, respectively [Jantas et al., 2008]. As shown by MTT reduction assay, UDA partially reduced the cell death induced by St (0.15 μM) and Dox (0.25 μM) at concentrations 10–20 μM and 10 μM in the St and Dox model, respectively (Fig. 1). The absolute EC_{50} value calculated using four concentration points in both models was around 0.1 μM (Table I). The range of protection mediated by UDA against St- and Dox-evoked cell death was comparable to the effect of caspase-3 inhibitor, Ac-DEVD-CHO (10 μM) (Fig. 1).

NEUROPROTECTION MEDIATED BY UDA AGAINST ST- AND DOX-TOXICITY IS EXECUTED BY CASPASE-3-INDEPENDENT MECHANISM ENGAGING AIF

Caspase-3 is one of the main executor of apoptotic process and its activation has been shown to be involved in St- and Dox-evoked cell

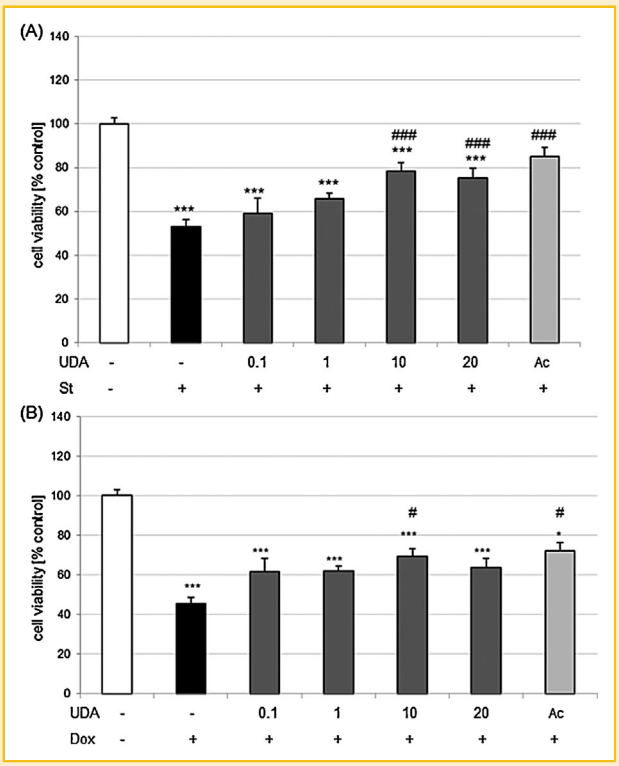

Fig. 1. UDA (10 and 20 μM) attenuates the staurosporine (St)- and doxorubicin (Dox)-evoked cell damage in SH-SY5Y cells. The cells were treated with UDA (0.1–20 μM) or caspase-3 inhibitor (Ac-DEVD-CHO, 10 μM) and St (0.15 μM) or Dox (0.25 μM). After 24 h of treatment with agent, the cell viability was measured by MTT reduction assay. Data after normalization to vehicle-treated cells (100%) are presented as a mean ± SEM from three independent experiments with five replicates. $^{*}P < 0.05$ and $^{***}P < 0.001$ versus vehicle-treated cells; $^{\#}P < 0.05$ and $^{\#\#\#}P < 0.001$ versus St/Dox-treated cells.

TABLE I. The Estimation of EC_{50} Value for UDA Neuroprotective Effects in Various Model of SH-SY5Y Cell Injury

Models of cell damage	$LogEC_{50}$	EC_{50} [microM]	Concentration points
St	−1.493	0.102	4
Dox	−1.002	0.099	4
H_2O_2 for 6 h	−1.088	0.082	5
H_2O_2 for 24 h	−1.377	0.042	5

Absolute EC_{50} values for UDA neuroprotetive effects were calculated on the basis of data from cell viability measurement: St (Fig. 1A), Dox (Fig. 1B), H_2O_2 for 6 h (Fig. 4A) and 24 h (Fig. 4B) by using GraphPad Prism 5.04 software with log (agonist) versus normalized response analysis.

damage of SH-SY5Y cells [Jantas et al., 2008]. We measured caspase-3 activity after 9 h of treatment of SH-SY5Y cells with UDA (1-20 μM) and St (0.15 μM) and Dox (0.25 μM). We observed a significant increase in caspase-3 activity after St and Dox administration which was completely blocked by caspase-3 inhibitor, Ac-DEVD-CHO (10 μM). However, we did not observe any effect of UDA (1–20 μM) on basal and St- or Dox-induced caspase-3 activity (Table II).

Next, we studied the effect of UDA (1–20 μM) on St- and Dox-evoked changes in mitochondrial and cytosolic AIF protein level. We observed a significant reduction in mitochondrial (about 50%) and increase (about 3.5-fold) in cytosolic AIF level after 14 h of treatment of cells with St (0.15 μM) (Fig. 2A and B). The St-evoked changes in mitochondrial and cytosolic AIF level were partially attenuated by UDA at concentrations 10 and 20 μM, but not by 1 μM (Fig. 2A and B). In the Dox-model of SH-SY5Y cell injury, we observed about 20% reduction in mitochondrial and about 2.5-fold increase in cytosolic level of AIF after 18 h of treatment with this pro-apoptotic factor (Fig. 2C and D). UDA (10 μM) partially attenuated the Dox-evoked increase in cytosolic AIF level (Fig. 2D), being without influence on mitochondrial AIF level (Fig. 2C).

Further experiments demonstrated no significant reduction in $\Delta\Psi m$ after 9 h of treatment of cells with St (0.15 μM; $\Delta\Psi m = 99.99 \pm 4.35\%$) and Dox (0.25 μM; $\Delta\Psi m = 97.09 \pm 3.48\%$); thus, we excluded the mechanism of regulation of $\Delta\Psi m$ by UDA in its neuroprotective action against St- and Dox-evoked cell damage (data not shown). We also did not find any significant changes in ADP/ATP ratio after 18 h of treatment with St (0.15 μM) and Dox (0.25 μM) (the mean values for ADP/ATP ratio were control = 1.00 ± 0.17; St = 1.50 ± 0.22; Dox = 1.37 ± 0.20 [data not shown]) which suggests a predominance of apoptotic processes not connected with mitochondrial collapse in these models. Next, we tested the hypothesis about participation of ROS modulation in neuroprotective effects of UDA in the St and Dox model of cellular injury. First, we checked the ROS generation after 3–9 h of treatment of SH-SY5Y cells with St (0.15 μM) and Dox (0.25 μM) and showed that only St evoked a significant increase in CM-DCF fluorescence (Fig. 3A). However, UDA (1–40 μM) did not influence the St-evoked ROS production which in contrast was completely inhibited by NAC (0.5 mM) (Fig. 3B).

TABLE II. The Effects of UDA on St- and Dox-Induced Caspase-3 Activity in SH-SY5Y Cells

	Caspase-3 activity (% control)
Control	100.00 ± 1.26
UDA 10	98.12 ± 5.70
UDA 20	92.42 ± 3.61
St	748.87 ± 13.41***
+ Ac-DEVD-CHO	27.82 ± 2.74###
+ UDA 1	777.92 ± 15.89
+ UDA 10	744.06 ± 15.27
+ UDA 20	721.23 ± 7.71
Dox	530.53 ± 4.41***
+ Ac-DEVD-CHO	15.89 ± 2.85###
+ UDA 1	523.47 ± 26.99
+ UDA 10	550.45 ± 30.75
+ UDA 20	528.77 ± 18.59

The caspase-3 activity was measured after treatment of SH-SY5Y cells with UDA (1–20 uM), Ac-DEVD-CHO (10 uM) and staurosporine (St, 0.15 uM) or doxorubicin (Dox, 0.25 uM) for 9 h. Data were normalized to protein level and to vehicle-treated cells (100 %) and expressed as a mean ± SEM.
*** $P < 0.001$ versus vehicle-treated cells; ### $P < 0.001$ versus St/Dox-treated cells.

UDA INHIBITS THE H_2O_2-INDUCED CELL DAMAGE

We did not observe any cell damaging effect of UDA up to 40 μM after 6–24 h of incubation with SH-SY5Y cells as was confirmed by cell viability (MTT reduction) and toxicity (LDH release, PI staining) assays (Figs. 4 and 5). However, UDA (1–40 μM) reduced the cell death induced by H_2O_2 after 6 (H_2O_2 1 mM) and 24 h (H_2O_2 0.5 mM) of incubation with cells but its concentration of 0.1 μM was ineffective (Fig. 4). The absolute EC_{50} values calculated using five concentration points were 0.08 and 0.04 μM for 1 mM H_2O_2 and 0.5 mM H_2O_2, respectively (Table I). The range of protection mediated by UDA in cell viability assay (MTT reduction) after 6 h was comparable to the effect of calpain inhibitor, MDL28170 (10 μM), whereas after 24 h the protection mediated by UDA was slightly better than that mediated by MDL28170 (Fig. 4). Next, we confirmed the neuroprotective properties of UDA (1–40 μM) after 24 h of treatment in biochemical LDH release assay (Fig. 4A) and by using the necrotic marker, propidium ioide, and flow cytometry analysis of cells where UDA inhibited the H_2O_2-evoked increase in LDH release (Fig. 4A) and in the number of PI-positive nuclei (Fig. 4B). In contrast to MTT and LDH tests, the effects of UDA on H_2O_2-induced changes in PI test were dose-dependent (0.1–10 μM) (Fig. 5B).

UDA DIMINISHES THE H_2O_2-INDUCED CASPASE-3 AND CALPAIN ACTIVITY

We demonstrated a significant increase in caspase-3 activity after 9 h of treatment of cells with H_2O_2 (0.5 mM) which was completely blocked by its specific inhibitor, Ac-DEVD-CHO (10 μM) (Table II). UDA at concentrations of 10 and 20 μM, but not 1 μM partially attenuated the H_2O_2-induced caspase-3 activity (Fig. 6A). Next, by using semiquantitative Western blot analysis of 120 kDa spectrin α II breakdown product, which is specifically cleaved by caspases [Zhang et al., 2009; Jantas et al., 2011], we demonstrated the inhibition of H_2O_2-evoked increase in 120 kDa product by UDA (1–20 μM) after 9 h of treatment with the agents (Fig. 6B). Furthermore, by analyzing 145 kDa spectrin α II breakdown product, which is specifically cleaved by calpain, we demonstrated lower intensity bands after treatment of cells with H_2O_2 and UDA when compared to the group

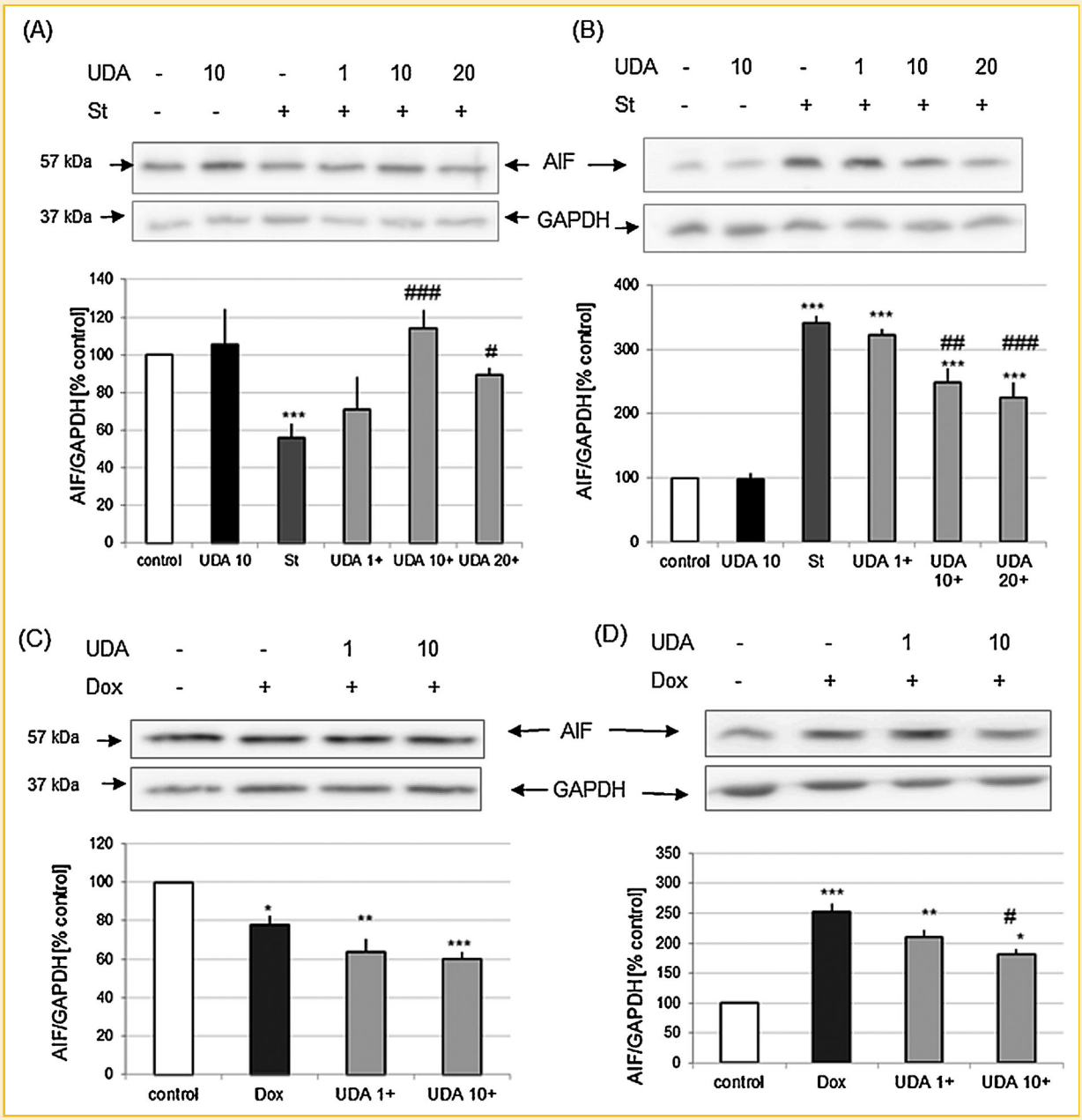

Fig. 2. (A and B) UDA (10 and 20 μM) prevents the changes in mitochondrial (A) and cytosolic (B) AIF level evoked by St. (C, D) UDA partially attenuates the Dox-induced increase in AIF cytosolic level (D) without influence on Dox-evoked reduction in mitochondrial AIF level (C). Bands show a Western blot (10% SDS–polyacrylamide gel) results of AIF mitochondrial (A) and cytosolic (B) level after treatment of cells with UDA (1–20 μM) and St (0.15 μM) or Dox (0.25 μM) for 14 and 18 h, respectively. Histograms show the optical density of bands of mitochondrial and cytosolic AIF level relative to GAPDH level (protein load control) from three separate experiments with two replicates. $^{*}P < 0.05$, $^{**}P < 0.01$, and $^{***}P < 0.001$ versus vehicle-treated cells; $^{\#}P < 0.05$, $^{\#\#}P < 0.01$ and $^{\#\#\#}P < 0.001$ versus St/Dox-treated cells.

treated only with H_2O_2 (Fig. 6B). UDA alone (20 μM) had no influence on the level of 145 and 120 kDA products when compared to vehicle-treated cells (Fig. 6B).

UDA DIMINISHES THE MITOCHONDRIAL DYSFUNCTIONS EVOKED BY H_2O_2

Previous studies showed that the H_2O_2-induced cell death was associated with a decrease in ΔΨm in SH-SY5Y cells (Natarajan and Becker, 2012; Richter et al., 2015). The present study showed that H_2O_2 (0.5 mM for 6 h) significantly decreased the ΔΨm when compared with the vehicle-treated cells (by about 30%) (Fig. 7A). While UDA treatment (10–40 μM) partially prevented the fall in ΔΨm induced by H_2O_2, the calpain inhibitor MDL28170 was without significant effect (Fig. 7A). In addition, there was no significant difference in TMRE fluorescence between the vehicle- and UDA (40 μM)-treated cells (Fig. 7A). Since changes in energetic status of

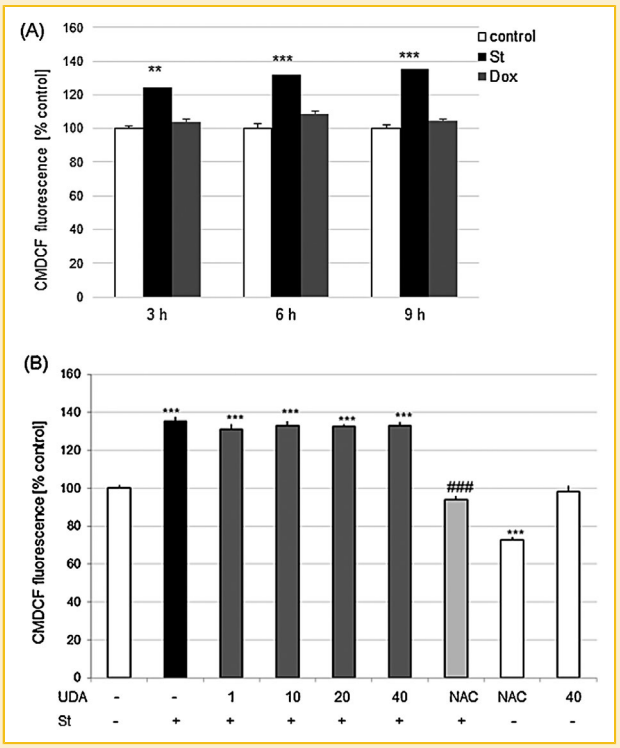

Fig. 3. UDA did not affect the staurosporine (St)-evoked increase in reactive oxygen species (ROS) level. (A) The study of the 3–9 h of treatment with St (0.15 μM) and doxorubicin (Dox, 0.25 μM) on ROS production. (B) The effect of UDA (1–40 μM) and antioxidant, N-acetylcysteine (NAC, 0.5 mM) on St-evoked increase in ROS production after 9 h of treatment with drugs. After cell treatment, cells were loaded with 10 μM of CM-H_2DFFDA for 30 min and fluorescence was measured in multi-well plate-reader. Data after normalization to fluorescence in vehicle-treated cells (100%) are presented as a mean ± SEM from three independent experiments with five replicates. $^{**}P < 0.01$ and $^{***}P < 0.001$ versus vehicle-treated cells; $^{###}P < 0.001$ versus St-treated cells.

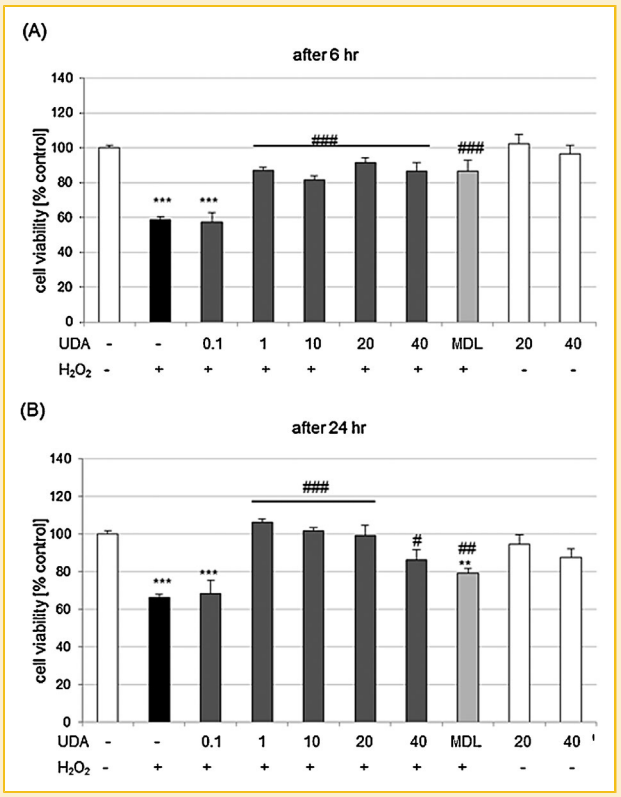

Fig. 4. UDA (1–40 μM) prevents the hydrogen peroxide (H_2O_2)-evoked reduction in cell viability after 6 (A) and 24 h (B) incubation of cells with agents. The cells were treated with UDA (0.1–40 μM) or calpain inhibitor, MDL28170 (10 μM), and H_2O_2 (1 and 0.5 mM for 6 and 24 h, respectively) followed by cell viability measurement (MTT reduction assay). Data after normalization to vehicle-treated cells (100%) are presented as a mean ± SEM from three independent experiments with five replicates. $^{**}P < 0.01$ and $^{***}P < 0.001$ versus vehicle-treated cells; $^{#}P < 0.05$, $^{##}P < 0.01$, and $^{###}P < 0.001$ versus H_2O_2-treated cells.

cells (ADP/ATP ratio) are commonly used to assess not only the mode of cell death (apoptotic vs. necrotic) but also the influence of the tested neuroprotectants on this parameter, in the next part of the study, we evaluated the effect of UDA (1 and 10 μM) and H_2O_2 (0.5 mM) on ADP/ATP ratio after 18 h of incubation with the agents. We showed about 2.5-fold increase in ADP/ATP ratio after H_2O_2 treatment which was partially attenuated by UDA at concentration 10 μM but not 1 μM (Fig. 7B).

UDA PREVENTS THE CHANGES IN MITOCHONDRIAL AND CYTOSOLIC AIF LEVEL EVOKED BY H_2O_2

Since previous studies demonstrated the participation of AIF translocation in execution of apoptotic cell death in cells exposed to oxidative stress [Son et al., 2009; Doti et al., 2014], we verified this mechanism in neuroprotection mediated by UDA against H_2O_2-evoked cell death by measuring the mitochondrial and cytosolic level of AIF. We observed a significant reduction in mitochondrial (about 40%) and increase (about 3-fold) in cytosolic AIF level after 14 h of treatment of cells with H_2O_2 (0.5 mM) (Fig. 7C and D). The H_2O_2-evoked changes in mitochondrial and cytosolic AIF level were reduced by UDA, however, differed in the level of effective concentrations which was 10 μM for mitochondrial and 1 and 10 μM for cytosolic cell fractions (Fig. 7C and D).

UDA PARTIALLY ATTENUATES THE H_2O_2-INDUCED ROS GENERATION BUT ONLY AT ITS HIGHER CONCENTRATION

H_2O_2 was reported previously to generate an excessive amount of reactive oxygen species (ROS) in SH-SY5Y cells which could be responsible for execution of cell death via apoptotic-necrotic mechanisms [Son et al., 2009; Lee et al., 2012; Taki-Nakano et al., 2014]. The present study revealed that administration of H_2O_2 (0.5 mM) for 1 h into cells preloaded with CM-H_2DCFDA (10 μM) evoked about 3-fold increase in CM-DCF fluorescence when compared with the vehicle-treated cells (Fig. 8). Treatment of cells with UDA at a concentration of 40 μM, but not 0.1–20 μM, partially attenuated the H_2O_2-evoked increase in CM-DCF oxidation assay (Fig. 8). N-Acetylcysteine (NAC, 0.5 mM), a precursor of the antioxidant glutathione, almost completely blocked the H_2O_2-induced increase in

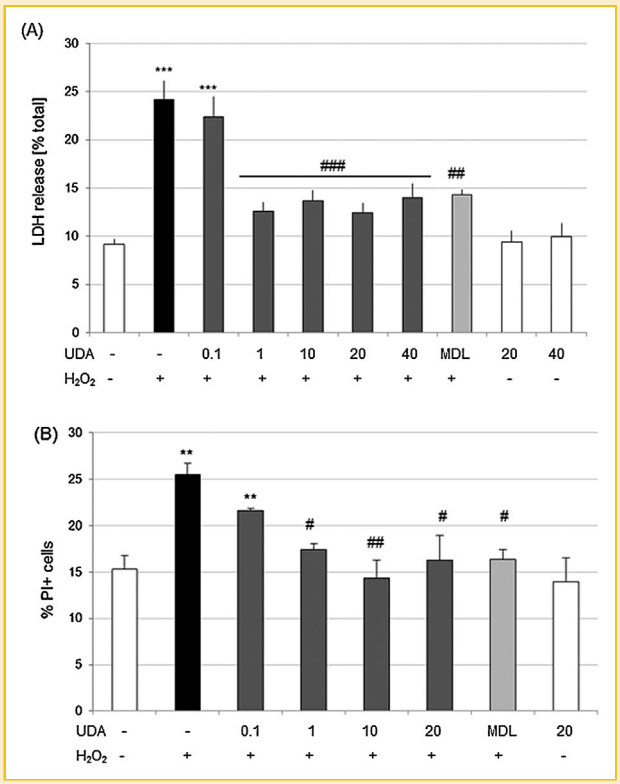

Fig. 5. (A) UDA (1–40 μM) prevents the hydrogen peroxide (H_2O_2)-induced LDH release. The cells were treated with UDA (0.1–40 μM) or calpain inhibitor, MDL28170 (10 μM), and H_2O_2 (0.5 mM) for 24 h. LDH activity was measured in culture medium derived from drug treated cells. Data after normalization to total LDH release ($TritonX_{100}$-treated cells, 100%) are presented as a mean ± SEM from three independent experiments with five replicates. (B) UDA (1–20 μM) diminishes the H_2O_2-evoked increase in the number of necrotic nuclei. The cells were treated with UDA (0.1–20 μM) or calpain inhibitor, MDL28170 (10 μM), and H_2O_2 (0.5 mM) for 24 h, stained with of propidium ioide (PI) and analyzed by flow cytometry (Details in Materials and Methods). Data are shown as a percentage of PI-positive cells (mean ± SEM) from three independent experiments with three replicates. $^{**}P < 0.01$ and $^{***}P < 0.001$ versus vehicle-treated cells; $^{\#}P < 0.05$, $^{\#\#}P < 0.01$ and $^{\#\#\#}P < 0.001$ versus H_2O_2-treated cells.

CM-DCF fluorescence, whereas calpain inhibitor, MDL28170 was without a significant effect (Fig. 8A).

THE NEUROPROTECTION MEDIATED BY UDA IN VARIOUS MODELS OF SH-SY5Y CELL INJURY IS BLOCKED BY PI3-K/AKT INHIBITOR

Activation of pro-survival PI3-K/Akt and/or MAPK/ERK1/2 pathways often contributes to the mechanism of neuroprotection mediated by various kinds of drugs [Hetman and Gozdz, 2004; Burke, 2007; Ahn, 2014; Jantas et al., 2014]. Thus, we tested the effect of the inhibitor of PI3-K/Akt pathway, LY294002 (10 μM) and of MAPK/ERK1/2 route, U0126 (10 μM) on neuroprotection mediated by UDA (10 μM) in various models of SH-SY5Y cell injury. We demonstrated that a 30-min pretreatment of SH-SY5Y cells with LY294002, but not with U0126 blocked the neuroprotection mediated by UDA against cell death evoked by H_2O_2, St, and Dox (Table III) as confirmed by cell viability assay. We observed the increase in cell death after LY294002 and H_2O_2 treatment when compared to the effect of H_2O_2, whereas we did not notice any influence of this inhibitor on St- and Dox-evoked reduction in cell viability (Table III). U0126 did not affect the extent of cell damage induced by H_2O_2, St, or Dox (Table III).

DISCUSSION

We studied the neuroprotective potential of UDA and its mechanisms of action in apoptotic and oxidative stress models of cell injury in human neuroblastoma SH-SY5Y cells. The main results of the present study demonstrated that (i) UDA partially attenuated the cell death induced by St and Dox via a caspase-3-independent mechanism; (ii) UDA prevented the cell death induced by H_2O_2 via inhibition of necrotic and apoptotic processes; and (iii) activation of PI3-K/Akt pathway was responsible for neuroprotection mediated by UDA against pro-apoptotic factors- and oxidative stress-induced cell death.

The results of our study for the first time showed the protective potential of UDA against the cell damage evoked by St- and Dox, inducers of intracellular (mitochondrial) and extracellular (death receptor mediated) apoptotic pathway, respectively [Jantas et al., 2008]. The magnitude of protection mediated by UDA against pro-apoptotic factors-induced cell damage was relatively smaller (Fig. 1) than that against H_2O_2 (Fig. 4). Our results on neuroprotection of UDA against oxidative stress-induced cell death in SH-SY5Y cells not only confirm the data reported by Lee et al. [2012] who demonstrated the neuroprotective potential of UDA (20 μM) against SH-SY5Y cell death induced by H_2O_2, amyloid β, and glutamate, but also provide a novel evidence for mechanisms involved. In our study, we tested a wide range of concentrations of UDA (0.01–40 μM) to better characterize its pharmacological profile and we used two concentrations of H_2O_2 to model acute (1 mM for 6 h) and prolonged (0.5 mM for 24 h) oxidative stress-dependent neurodegenerative conditions which could be manifested by prevalence of necrotic or apoptotic-necrotic processes, respectively [Son et al., 2009; Piotrowski et al., 2013; Richter et al., 2015]. By using the MTT reduction cell viability assay, we showed in both models a relatively good neuroprotective response to UDA in a wide range of concentrations (1–40 μM) which in the acute model was comparable with neuroprotection mediated by the calpain inhibitor MDL28170, but in the prolonged oxidative stress model, the protection mediated by UDA was relatively better than that of the latter one (Fig. 4). These differences could be explained by the fact that acute oxidative stress evokes a rapid increase in intracellular calcium level which activates mainly calpains, whereas in the prolonged model of oxidative stress, an activation of apoptotic processes occurs via activation of caspase-3-dependent and -independent mechanisms [Sanvicens et al., 2006; Son et al., 2009; Richter et al., 2015]. In contrast to our study, Lee et al. [2012] did not find protection mediated by MDL28170 (20 μM) against the H_2O_2 (2 mM)-evoked cell death as they used one cell viability assay (kit-8 solution). In our study, apart from using general

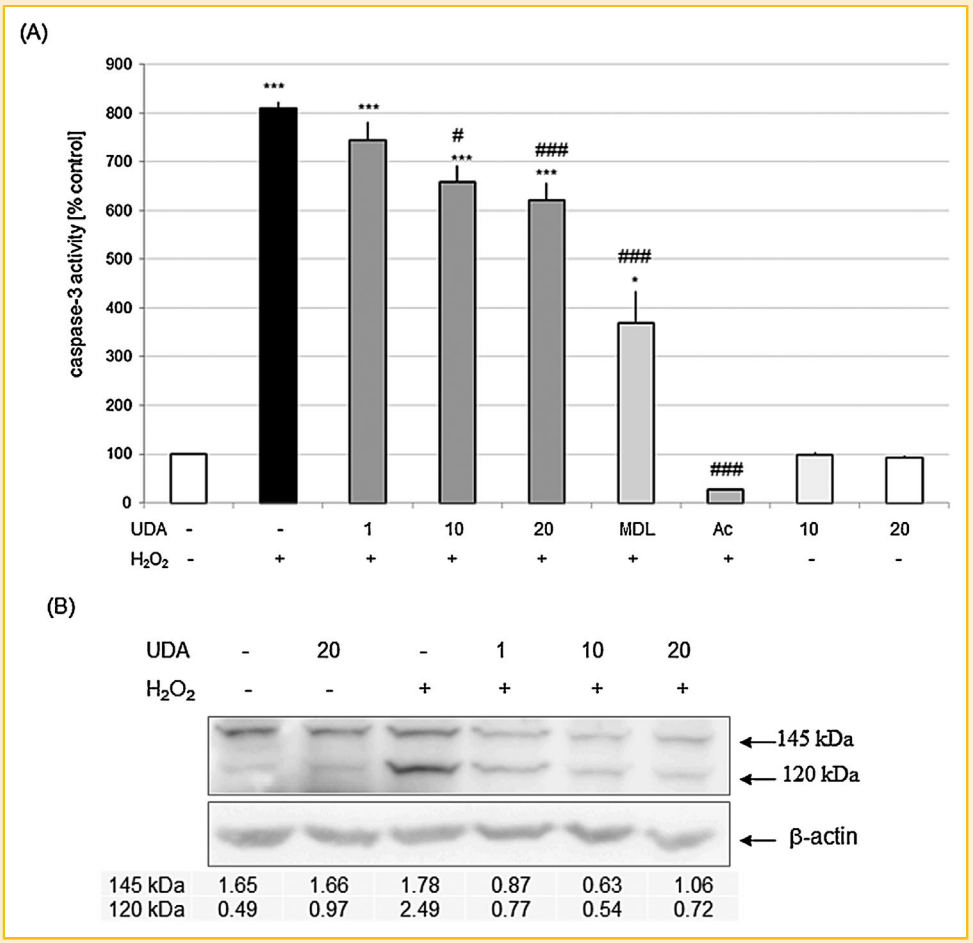

Fig. 6. (A) UDA (10 and 20 μM) attenuates the H_2O_2-induced caspase-3 activity. The cells were treated with UDA (1–20 μM), caspase-3 inhibitor (AcDEVD-CHO, 10 μM), calpain inhibitor (MDL28170, 10 μM), and H_2O_2 (0.5 mM) for 9 h. The enzyme activity was measured by using biochemical assay with Ac-DEVD-AMC substrate, which is specifically cleaved by caspase-3. Data were normalized to protein level and to vehicle-treated cells (100%) and expressed as a mean ± SEM from three independent experiments with two replicates. $^{***}P < 0.001$ versus vehicle-treated cells; $^{\#}P < 0.05$ and $^{\#\#\#}P < 0.001$ versus H_2O_2-treated cells. (B) UDA (1–20 μM) inhibits calpain and caspase-3 activity measured by Western blot analysis of spectrin α II breakdown products 145 and 120 kDa. The cells were treated with UDA (1–20 μM) and H_2O_2 (0.5 mM) for 9 h and an equal amount of protein from experimental groups was separated on 7% SDS–polyacrylamide gel, transferred onto a PVDF membrane, stained with specific antibodies, and detected by chemiluminescence method. Data from optical density readouts for 145 and 120 kDa bands for each treatment group were normalized to β-actin level.

cell viability assay (MTT reduction), in the prolonged oxidative stress model, we confirmed the protection mediated by UDA (1–40 μM) and MD28170L by biochemical cell toxicity assay (LDH release) and flow cytometry analysis of PI-positive cells (Fig. 5), which are the common markers for cell membrane integrity loss. Since UDA belongs to the group of monounsaturated fatty acids, thus, in the next part of the study, we evaluated the ability of UDA to directly scavenge H_2O_2-induced reactive oxygen species (ROS). Since, only the highest concentration of UDA tested (40 μM) attenuated the H_2O_2-induced CM-DCF fluorescence (Fig. 8) and neuroprotective response was observed for a wider range of concentrations (1–40 μM) (Figs. 4 and 5), we excluded the contribution of direct ROS scavenging properties of UDA to the mechanisms of its neuroprotective effects found in oxidative stress model. Since we did not find any attenuation of St-evoked increase in ROS generation by UDA (1–40 μM), we also excluded this mechanism as contributing to neuroprotective response found in the St model of cell damage (Fig. 3). Our observation from oxidative stress model is in contrast to the study by Lee et al. [2012] who showed the decrease in H_2O_2-induced ROS generation after UDA (20 μM) and MDL28170 (20 μM) treatment with the higher effectiveness of the latter one. These discrepancies between our and Lee et al. [2012] studies could be explained by different scheme of cell treatment for ROS measurement and different fluorescent probes used in both studies. In our co-treatment study with H_2O_2 and UDA/MDL28170 for 1 h which was preceded by cell loading with ROS indicator, CM-H_2DCFDA, we estimated a rather direct effect of the tested agents on ROS formation. In contrast, Lee at al. [2012] used 24 h pre-treatment with UDA and MDL28170 followed by exposure of cells to H_2O_2 (0.4 mM) for 5–20 min and then cells were loaded with ROS marker, DCFH2-DA. This method could rather detect an indirect effect of the tested neuroprotective compounds for example via increased expression of endogenous antioxidant systems. To this end, previous chemical screening study for antioxidant activities of several commercially

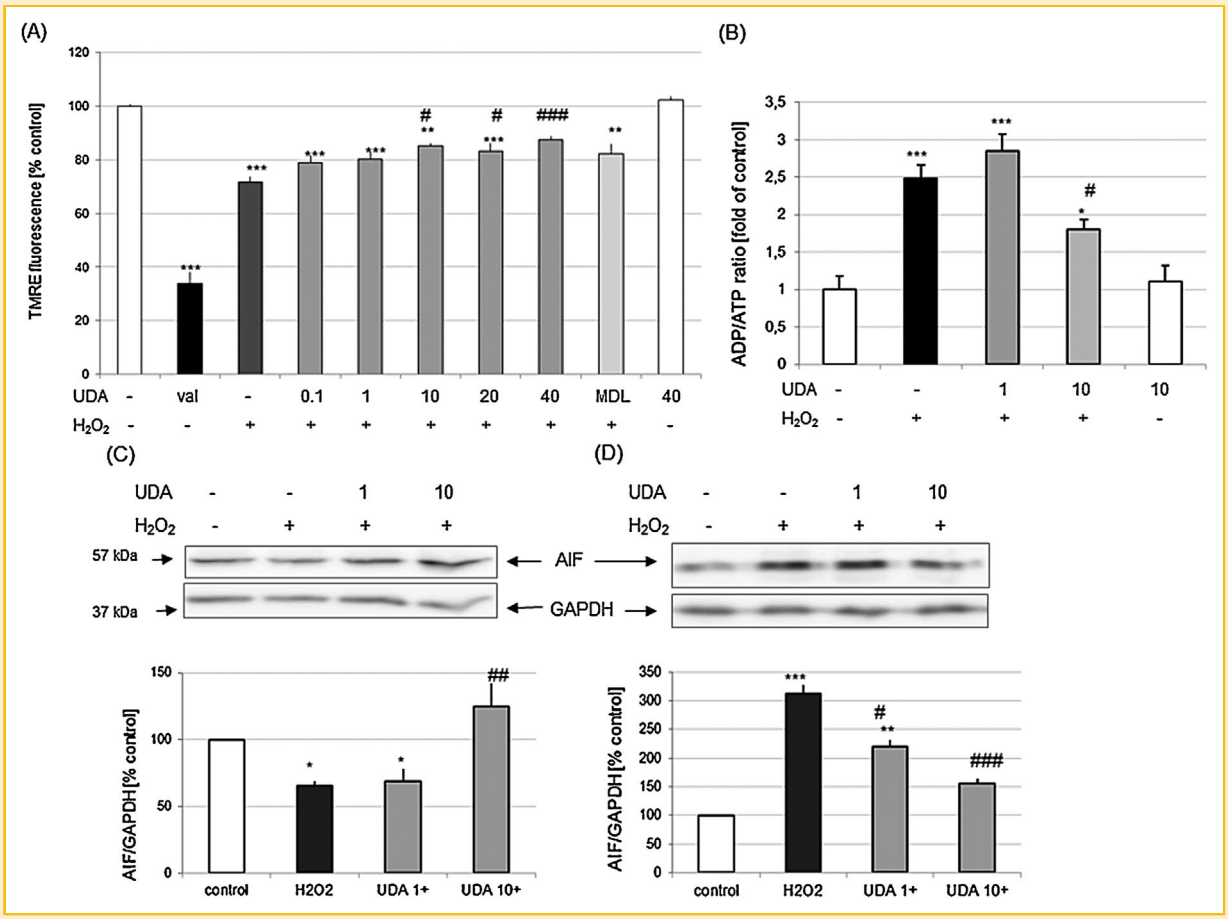

Fig. 7. (A) UDA (10–40 μM) partially prevents the reduction in mitochondrial membrane potential evoked by H_2O_2 in SH-SY5Y cells. The cells were treated with UDA (0.1–40 μM), calpain inhibitor (MDL28170, 10 μM), and H_2O_2 (0.5 mM) for 6 h. Valinomycin (val, 10 μM for 5 min), a mitochondria depolarizating agent, was used as a positive control for the assay. After treatment, the cells were loaded with TMRE (100 nM) for 30 min and the fluorescence was measured in microplate fluorescence reader. Data after normalization to vehicle-treated cells (100%) are presented as a mean ± SEM from three independent experiments with five replicates. (B) UDA (10 μM) attenuates the H_2O_2-induced increase in ADP/ATP ratio. The cells were treated with UDA (1 and 10 μM) and H_2O_2 (0.5 mM) for 18 h and ADP/ATP ratio was estimated by specific bioluminescent assay (EnzyLightTM ADP/ATP Ratio Assay Kit, BioAssay Systems). Calculated ADP/ATP ratio is shown as a mean ± SEM from two independent experiments with three replicates. (C and D) UDA reduces the H_2O_2-evoked changes in mitochondrial (C) and cytosolic (D) AIF level. Bands show a Western blot (10% SDS–polyacrylamide gel) results of AIF mitochondrial (C) and cytosolic (D) level after treatment of cells with UDA (1 and 10 μM) and H_2O_2 (0.5 mM) for 14 h. Histograms show the optical density of bands of mitochondrial and cytosolic AIF level relative to GAPDH level (protein load control) from three separate experiments with two replicates. $^{*}P < 0.05$, $^{**}P < 0.01$, and $^{***}P < 0.001$ versus vehicle-treated cells; $^{\#}P < 0.05$, $^{\#\#}P < 0.01$, and $^{\#\#\#}P < 0.001$ versus H_2O_2-treated cells.

available C-8 to C-24 saturated and unsaturated fatty acids (1–29) demonstrated that among all tested compounds at concentrations 60 μG/mL(−1) only UDA with two other unsaturated fatty acids (cis-5-dodecenoic acid and nervonic acid) were devoid of such activity [Henry et al., 2002].

Searching for other putative neuroprotective mechanisms which could underlie UDA activity against pro-apoptotic factors—and oxidative stress-evoked cell damage, we demonstrated its ability to attenuate the H_2O_2—but not St or Dox-induced caspase-3 activity (Fig. 6, Table II). These results, to some extent, could explain lower neuroprotective efficiency of UDA observed in St and Dox model in comparison to H_2O_2 one. Additionally, we confirmed the attenuating effect of UDA (1–20 μM) on H_2O_2-evoked caspase-3 activity by indirect method, by using WB analysis of 120 kDa spectrin α II breakdown product which is specifically cleaved by caspases. Moreover, we showed the attenuating effect of UDA (1–20 μM) on 145 kDa spectrin α II product which is specifically cleaved by calpain (Fig. 4B). The above findings are in line with data published by Lee et al. [2012] who showed the attenuating effect of UDA (20 μM) on glucose-oxidation-evoked increase in calpain and caspase-3 activity in the model of continuous oxidative stress, measured by WB analysis of p25 cleavage product of p35 and cleaved caspase-3 and PARP, respectively. Moreover, in our study, we proposed new mechanisms responsible for neuroprotection mediated by UDA against H_2O_2-evoked cell death by showing its influence on mitochondrial function. By demonstration that UDA partially prevented the oxidative-stress-evoked fall in $\Delta\Psi m$ and increase in ADP/ATP ratio (Fig. 7), we suggest that mitochondria could be one of important players in neuroprotection mediated by UDA at least in the model of cell death executed by apoptotic-necrotic mechanism.

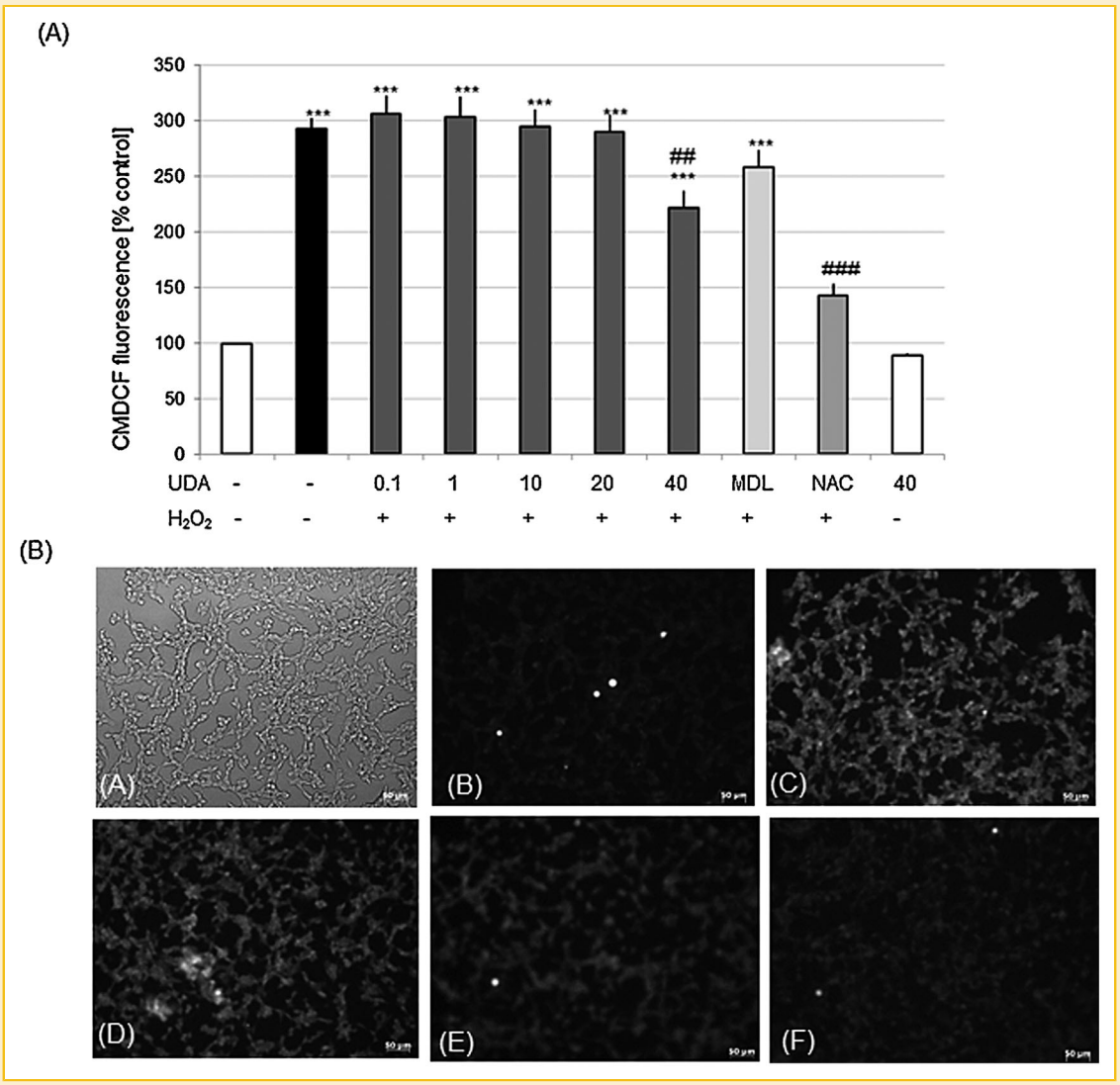

Fig. 8. (A) UDA (40 μM) partially reduces the H_2O_2-evoked increase in reactive oxygen species (ROS) level. ROS production was assayed by loading SH-SY5Y cells with 5 μM of CM-H_2DFFDA for 30 min. The cells were then treated with UDA (0.1–40 μM), calpain inhibitor (MDL28170, 10 μM), antioxidant (N-acetylcysteine, 0.5 mM), and H_2O_2 (0.5 mM) for 1 h and fluorescence of CM-DCF was measured in multi-well plate-reader. Data after normalization to fluorescence in vehicle-treated cells (100%) are presented as a mean ± SEM from three independent experiments with five replicates. $^{***}P < 0.001$ versus vehicle-treated cells; $^{\#\#}P < 0.01$ and $^{\#\#\#}P < 0.001$ versus H_2O_2-treated cells. (B) Microphotographs of vehicle-treated SH-SY5Y cells taken under differential interference contrast (DIC) method (A) and cells loaded with CM-H2DFFDA and treated for 1 h with vehicle (B), H_2O_2 (C), H_2O_2 + UDA 10 μM (D), H_2O_2 + UDA 40 μM (E), and H_2O_2 + NAC (F).

Further investigation of apoptosis inducing factor (AIF) mitochondrial-nuclear translocation, which is responsible for caspase-independent large scale DNA fragmentation [Daugas et al., 2000; Joza et al., 2009], revealed a UDA-induced modulation of St- and H_2O_2-evoked changes in mitochondrial and cytosolic AIF level (Figs. 2 and 7C and D), whereas in the Dox-model, we observed the protective effect of UDA only on its cytosolic level (Fig. 2). Our data not only confirmed the previous findings about participation of AIF translocation in the St-, Dox-, and H_2O_2-induced cell damage in various cellular systems, including SH-SY5Y cells [Yuste et al., 2005; Beart et al., 2007; Son et al., 2009; Doti et al., 2014; Jantas et al., 2015; Richter et al., 2015] but showed for the first time the ability of UDA to prevent these changes. It is not excluded that the modulation by UDA of various steps in apoptotic cell death machinery induced via mitochondrial (St and H_2O_2) and extracellular (Dox) pathways are responsible for the increase in AIF mitochondrial level induced by UDA in St and H_2O_2 models, observed in our study, and lack of changes in the Dox model (Fig. 2 and 8); however, this hypothesis needs further investigation. Regarding the participation of inhibition of AIF translocation in neuroprotection mediated by fatty acids, it has been shown that that mechanism is involved in neuroprotective effect of docosahexaenoic acid (DHA, 20 μM), a major dietary ω-3 long-chain polyunsaturated fatty acids (PUFA), against oxidative/genotoxic stress induced by MNNG (N-methyl-N′-nitro-N-nitrosoguanidine) in neuronal HT-22

TABLE III. The Effects of PI3-K/Akt and MAPK/ERK1/2 Inhibitors on Neuroprotection Mediated by UDA Against St-, Dox-, and H_2O_2-Induced Cell Death in SH-SY5Y Cells

	Cell viability (% control)
Control	100.00 ± 2.03
St	53.66 ± 1.89***
+ UDA	78.20 ± 2.80***, $^{###}$
+ LY294002 + UDA	48.02 ± 2.14***, ^{ααα}
+ U0126 + UDA	65.91 ± 3.30***, $^{#}$
+ LY294002	52.62 ± 4.81***
+ U0126	49.29 ± 1.57***
Dox	51.85 ± 1.99***
+ UDA	67.63 ± 1.65***, $^{###}$
+ LY294002 + UDA	47.34 ± 2.44***, ^{ααα}
+ U0126 + UDA	63.70 ± 5.81***, $^{##}$
+ LY294002	45.78 ± 1.74***
+ U0126	46.60 ± 4.94***
H_2O_2	56.07 ± 1.84***
+ UDA	81.63 ± 2.85***, $^{###}$
+ LY294002 + UDA	48.97 ± 2.02***, ^{ααα}
+ U0126 + UDA	71.06 ± 4.28***, $^{##}$
+ LY294002	42.42 ± 2.82***, $^{#}$
+ U0126	53.97 ± 3.40***

The cells were pretreated for 30 min with PI3-K/Akt, LY294002 (10 uM), or MAPK/ERK1/2, U0126 (10 uM) inhibitors followed by 24 h incubation of cells with UDA (10 uM) and cell damaging factors (St, 0.15 uM; Dox, 0.25 uM and H_2O_2, 0.5 mM). Cell viability was measured by MTT reduction assay and data after normalization to vehicle-treated cells (100 %) were presented as a mean±SEM from three independent experiment with five repetitions in each.
$^{***}P < 0.001$ versus vehicle-treated cells; $^{#}P < 0.05$, $^{##}P < 0.01$, and $^{###}P < 0.001$ versus St/Dox/H_2O_2-treated cells; $^{ααα}P < 0.001$ versus St/Dox/H2O2 + UDA-treated cells.

cells [Cieslik et al., 2013]. Based on our data and the above-mentioned study, it can be speculated that inhibition of AIF translocation could be a common neuroprotective mechanism mediated by MUFAs and PUFAs. On the other hand, it has been shown that the inhibition of caspase-3 is involved in neuroprotection mediated by some PUFAs, DHA, and EPA against the St-evoked cell damage in neuroblastoma Neuro2A cells and NRK-52E; however, AIF translocation was not measured in these studies (Akbar and Kim, 2002; Taneda et al., 2010). Contrary to neuroprotective effectiveness of unsaturated fatty acids, there is also a line of reports demonstrating a chemopreventive and chemosensitizer effects of dietary available PUFAs (e.g., eleostearic acid, lipoic acid, EPA, DHA) in various cell lines with induction of caspase-3-dependent and -independent mechanisms [Plumb et al., 1993; Reynolds et al., 2001; Rudra and Krokan, 2001; Hardman, 2004; Lindskog et al., 2006]. Moreover, the direct influence of PUFA on chemical-physical changes in cell membrane microdomains after DHA and EPA incorporation has been suggested to be involved in anti-proliferative and pro-apototic action of these compounds in breast cancer cells [Corsetto et al., 2012]. However, till now, there is no data demonstrating chemopreventive or chemosensitizer effects of UDA, which rather suggests that with respect to neuroprotection this compound could be relatively safer when compared to PUFA.

In the last part of our study, we demonstrated that the inhibitor of PI3-K/Akt pathway, LY294002 but not MAPK/ERK1/2 path, U0126 reversed the protection mediated by UDA against the oxidative-stress- and pro-apoptotic factors-induced SH-SY5Y cell damage (Table III). Since previous studies demonstrated the inhibition of PI3-K/Akt signaling by staurosporine (protein kinase inhibitor) or doxorubicin in various cells including SH-SY5Y one [Akbar and Kim, 2002; Heo et al., 2009; Jantas et al., 2008, 2009; Teng and Tang, 2013; Yu et al., 2013], it was expected that activation of this pro-survival pathway could be involved in the UDA-mediated protection against St- and Dox-evoked cell damage. However, in the case of H_2O_2-evoked cell damage, the data rather show a rapid induction of PI3-K/Akt pathway after H_2O_2 exposure which diminishes with time [Ruffels et al., 2004; Sanvicens et al., 2006; Que et al., 2013] suggesting induction of endogenous protective response against oxidative stress. This could be further evidenced by the fact that PI3-K/Akt inhibitor did not inhibit but increased the cell death induced by H_2O_2 in our and others' studies (Ruffels's et al., 2004; Sanvicens et al., 2006). Nevertheless, in our study, we demonstrated for the first time that in various models of SH-SY5Y cell injury, an induction of PI3-K/Akt pathway is crucial for neuroprotective action of UDA. The activation of PI3-K/Akt pathway by various factors could prevent cellular demise at various steps of cell death machinery [Burke, 2007; Son et al., 2009; Ahn, 2014]; however, the extent of this protection seems to be specific for the used cell-damaging factors. This could be exemplified by our study, where we observed blockade of UDA-mediated protection in all tested model of cell damage (H_2O_2, St, and Dox) by the PI3-K/Akt inhibitor, LY294002 but in dependence on the studied model of cell injury we demonstrated the participation of various mechanisms (caspase-3 dependent and/or -independent). The participation of PI3-K/Akt pathway activation has been proposed previously as an important mechanisms for PUFA-mediated neuroprotection [Michael-Titus and Priestley, 2014; Haast and Kiliaan, 2015]. For example, it has been shown that protection mediated by DHA against the St-evoked cell damage in Neuro 2A cells engage PI3-K/Akt activation [Akbar and Kim, 2002]. PI3-K/Akt activation regulates many early and late steps in apoptotic cell death machinery with its inhibitory effect on both caspase-3-dependent and -independent processes (Burke, 2007; Ahn, 2014). To this end, it has been shown that SH-SY5Y cells with overexpressed active PKB/Akt or Bcl-2 were resistant for ceramide-induced cell damage via mechanism connected with inhibition of AIF translocation [Kim et al., 2007].

Summing up, the present study showed that UDA could be neuroprotective against the pro-apoptotic factors- and oxidative stress-evoked cell death in human neuroblastoma SH-SY5Y via caspase-3-dependent and/or -independent mechanisms. Moreover, an activation of PI3-K/Akt pathway and influence on AIF translocation seems to be a common protective mechanism of UDA in all tested models of cell damage. Altogether, these results give rationale for further investigation of UDA neuroprotective potential in animal models of neurodegeneration.

ACKNOWLEDGMENTS

The study was supported by statutory funds of the Institute of Pharmacology, Polish Academy of Sciences, and the Polish-Norwegian Research Programme operated by the National Centre for Research and Development under the Norwegian Financial Mechanism 2009–2014 in the framework of Project Contract No. Pol-Nor/199523/64/2013 NanoNeucar. We kindly thank Ms. Barbara Korzeniak for her excellent technical assistance.

REFERENCES

Ahn JY. 2014. Neuroprotection signaling of nuclear akt in neuronal cells. Exp Neurobiol 23:200–206.

Almeida PV, Shahbazi MA, Mäkilä E, Kaasalainen M, Salonen J, Hirvonen J, Santos HA. 2014. Amine-modified hyaluronic acid-functionalized porous silicon nanoparticles for targeting breast cancer tumors. Nanoscale 6:10377–10387.

Akbar M, Kim HY. 2002. Protective effects of docosahexaenoic acid in staurosporine-induced apoptosis: Involvement of phosphatidylinositol-3 kinase pathway. J Neurochem 82:655–665.

Beart PM, Lim ML, Chen B, Diwakarla S, Mercer LD, Cheung NS, Nagley P. 2007. Hierarchical recruitment by AMPA but not staurosporine of pro-apoptotic mitochondrial signaling in cultured cortical neurons: Evidence for caspase-dependent/independent cross-talk. J Neurochem 103:2408–2427.

Brayden DJ, Walsh E. 2014. Efficacious intestinal permeation enhancement induced by the sodium salt of 10-undecylenic acid, a medium chain fatty acid derivative. AAPS J 16:1064–1076.

Burke RE. 2007. Inhibition of mitogen-activated protein kinase and stimulation of Akt kinase signaling pathways: Two approaches with therapeutic potential in the treatment of neurodegenerative disease. Pharmacol Ther 114:261–277.

Cieslik M, Pyszko J, Strosznajder JB. 2013. Docosahexaenoic acid and tetracyclines as promising neuroprotective compounds with poly(ADP-ribose) polymerase inhibitory activities for oxidative/genotoxic stress treatment. Neurochem Int 62:626–636.

Corsetto PA, Cremona A, Montorfano G, Jovenitti IE, Orsini F, Arosio P, Rizzo AM. 2012. Chemical-physical changes in cell membrane microdomains of breast cancer cells after omega-3 PUFA incorporation. Cell Biochem Biophys 64:45–59.

Daugas E, Susin SA, Zamzami N, Ferri KF, Irinopoulou T, Larochette N, Prévost MC, Leber B, Andrews D, Penninger J, Kroemer G. 2000. Mitochondrio-nuclear translocation of AIF in apoptosis and necrosis. FASEB J 14:729–739.

Doti N, Reuther C, Scognamiglio PL, Dolga AM, Plesnila N, Ruvo M, Culmsee C. 2014. Inhibition of the AIF/CypA complex protects against intrinsic death pathways induced by oxidative stress. Cell Death Dis 5:e993.

Haast RA, Kiliaan AJ. 2015. Impact of fatty acids on brain circulation, structure and function. Prostaglandins Leukot Essent Fatty Acids 92C: 3–14.

Halliwell B, Whiteman M. 2004. Measuring reactive species and oxidative damage in vivo and in cell culture: How should you do it and what do the results mean? Br J Pharmacol 142:231–255.

Hardman WE. 2004. (n-3) fatty acids and cancer therapy. J Nutr 134:3427S–3430S.

Hashem MA, Jun KY, Lee E, Lim S, Choo HY, Kwon Y. 2008. A rapid and sensitive screening system for human type I collagen with the aim of discovering potent anti-aging or anti-fibrotic compounds. Mol Cells 26:625–630.

Henry GE, Momin RA, Nair MG, Dewitt DL. 2002. Antioxidant and cyclooxygenase activities of fatty acids found in food. J Agric Food Chem 50:2231–2234.

Heo SR, Han AM, Kwon YK, Joung I. 2009. P62 protects SH-SY5Y neuroblastoma cells against H2O2-induced injury through the PDK1/Akt pathway. Neurosci Lett 450:45–50.

Hetman M, Gozdz A. 2004. Role of extracellular signal regulated kinases 1 and 2 in neuronal survival. Eur J Biochem 271:2050–2055.

Jantas D, Pytel M, Mozrzymas JW, Leskiewicz M, Regulska M, Antkiewicz-Michaluk L, Lason W. 2008. The attenuating effect of memantine on staurosporine-, salsolinol- and doxorubicin-induced apoptosis in human neuroblastoma SH-SY5Y cells. Neurochem Int 52:864–877.

Jantas D, Szymanska M, Budziszewska B, Lason W. 2009. An involvement of BDNF and PI3-K/Akt in the anti-apoptotic effect of memantine on staurosporine-evoked cell death in primary cortical neurons. Apoptosis 14:900–912.

Jantas D, Lorenc-Koci E, Kubera M, Lason W. 2011. Neuroprotective effects of MAPK/ERK1/2 and calpain inhibitors on lactacystin-induced cell damage in primary cortical neurons. Neurotoxicology 32:845–856.

Jantas D, Krawczyk S, Lason W. 2014. The predominant protective effect of tianeptine over other antidepressants in models of neuronal apoptosis: The effect blocked by inhibitors of MAPK/ERK1/2 and PI3-K/Akt pathways. Neurotox Res 25:208–225.

Jantas D, Greda A, Leskiewicz M, Grygier B, Pilc A, Lason W. 2015. Neuroprotective effects of mGluR II and III activators against staurosporine- and doxorubicin-induced cellular injury in SH-SY5Y cells: New evidence for a mechanism involving inhibition of AIF translocation. Neurochem Int. pii: S0197-0186(15) 00003-0 doi: 10.1016/j.neuint.2014.12.011. [Epub ahead of print].

Joza N, Pospisilik JA, Hangen E, Hanada T, Modjtahedi N, Penninger JM, Kroemer G. 2009. AIF: not just an apoptosis-inducing factor. Ann N Y Acad Sci. 1171:2–11.

Kang DH, Jun KY, Lee JP, Pak CS, Na Y, Kwon Y. 2009. Identification of 3-acetyl-2-aminoquinolin-4-one as a novel, nonpeptidic scaffold for specific calpain inhibitory activity. J Med Chem 52:3093–3097.

Kim MH, Shim KS, Lee SU, Kim YS, Min YK, Kim SH. 2010. Stimulatory effect of undecylenic acid on mouse osteoblast differentiation. Phytother Res 24:559–564.

Kim NH, Kim K, Park WS, Son HS, Bae Y. 2007. PKB/Akt inhibits ceramide-induced apoptosis in neuroblastoma cells by blocking apoptosis-inducing factor (AIF) translocation. J Cell Biochem 102:1160–1170.

Kovalainen M, Mönkäre J, Kaasalainen M, Riikonen J, Lehto VP, Salonen J, Herzig KH, Järvinen K. 2013. Development of porous silicon nanocarriers for parenteral peptide delivery. Mol Pharm 10:353–359.

Lee E, Eom JE, Kim HL, Kang DH, Jun KY, Jung DS, Kwon Y. 2012. Neuroprotective effect of undecylenic acid extracted from Ricinus communis L. through inhibition of μ-calpain. Eur J Pharm Sci 46:17–25.

Lindskog M, Gleissman H, Ponthan F, Castro J, Kogner P, Johnsen JI. 2006. Neuroblastoma cell death in response to docosahexaenoic acid: Sensitization to chemotherapy and arsenic-induced oxidative stress. Int J Cancer 118:2584–2593.

Lofrumento DD, La Piana G, Abbrescia DI, Palmitessa V, La Pesa V, Marzulli D, Lofrumento NE. 2011. Valinomycin induced energy-dependent mitochondrial swelling, cytochrome c release, cytosolic NADH/cytochrome c oxidation and apoptosis. Apoptosis 16:1004–1013.

Michael-Titus AT, Priestley JV. 2014. Omega-3 fatty acids and traumatic neurological injury: From neuroprotection to neuroplasticity? Trends Neurosci 37:30–38.

Monograph. 2002. Undecylenic acid. Altern Med Rev 7:68–70.[No authors listed].

Natarajan SK, Becker DF. 2012. Role of apoptosis-inducing factor, proline dehydrogenase, and NADPH oxidase in apoptosis and oxidative stress. Cell Health Cytoskelet. 2012(4):11–27.

Nieto A, Hou H, Moon SW, Sailor MJ, Freeman WR, Cheng L. 2015. Surface engineering of porous silicon microparticles for intravitreal sustained delivery of rapamycin. Invest Ophthalmol Vis Sci 56:1070–1080.

Piotrowski M, Szczepanowicz K, Jantas D, Leskiewicz M, Lason W, Warszynski P. 2013. Emulsion-core and polyelectrolyte-shell nanocapsules: Biocompatibility and neuroprotection against SH-SY5Y cells. J Nanopart Res 15:2035.

Que ZL, Zhou WJ, Chang J, Liu XH, Yu JM, Sun X. 2013. Neuroprotective effects of mercaptoethylleonurine and mercaptoethylguanidine analogs on hydrogen peroxide-induced apoptosis in human neuronal SH-SY5Y cells. Bioorg Med Chem Lett 23:1793–1796.

Plumb JA, Luo W, Kerr DJ. 1993. Effect of polyunsaturated fatty acids on the drug sensitivity of human tumour cell lines resistant to either cisplatin or doxorubicin. Br J Cancer 67:728–733.

Raku T, Kitagawa M, Shimakawa H, Tokiwa Y. 2003. Enzymatic synthesis of hydrophilic undecylenic acid sugar esters and their biodegradability. Biotechnol Lett 25:161–166.

Reynolds LM, Dalton CF, Reynolds GP. 2001. Phospholipid fatty acids and neurotoxicity in human neuroblastoma SH-SY5Y cells. Neurosci Lett 309:193–196.

Rhee SG, Chang TS, Jeong W, Kang D. 2010. Methods for detection and measurement of hydrogen peroxide inside and outside of cells. Mol Cells 29:539–549.

Richter M, Nickel C, Apel L, Kaas A, Dodel R, Culmsee C, Dolga AM. 2015. SK channel activation modulates mitochondrial respiration and attenuates neuronal HT-22 cell damage induced by H2O2. Neurochem Int 81:63–75.

Ruffels J, Griffin M, Dickenson JM. 2004. Activation of ERK1/2, JNK and PKB by hydrogen peroxide in human SH-SY5Y neuroblastoma cells: Role of ERK1/2 in H2O2-induced cell death. Eur J Pharmacol 483:163–173.

Rudra PK, Krokan HE. 2001. Cell-specific enhancement of doxorubicin toxicity in human tumour cells by docosahexaenoic acid. Anticancer Res 21:29–38.

Sanvicens N, Gómez-Vicente V, Messeguer A, Cotter TG. 2006. The radical scavenger CR-6 protects SH-SY5Y neuroblastoma cells from oxidative stress-induced apoptosis: Effect on survival pathways. J Neurochem 98:735–747.

Shahbazi MA, Almeida PV, Mäkilä EM, Kaasalainen MH, Salonen JJ, Hirvonen JT, Santos HA. 2014. Augmented cellular trafficking and endosomal escape of porous silicon nanoparticles via zwitterionic bilayer polymer surface engineering. Biomaterials 35:7488–7500.

Shrestha N, Shahbazi MA, Araújo F, Zhang H, Mäkilä EM, Kauppila J, Sarmento B, Salonen JJ, Hirvonen JT, Santos HA. 2014. Chitosan-modified porous silicon microparticles for enhanced permeability of insulin across intestinal cell monolayers. Biomaterials 35:7172–7179.

Son YO, Jang YS, Heo JS, Chung WT, Choi KC, Lee JC. 2009. Apoptosis-inducing factor plays a critical role in caspase-independent, pyknotic cell death in hydrogen peroxide-exposed cells. Apoptosis 14:796–808.

Tabasi O, Falamaki C, Khalaj Z. 2012. Functionalized mesoporous silicon for targeted-drug-delivery. Colloids Surf B Biointerfaces 98:18–25.

Taki-Nakano N, Ohzeki H, Kotera J, Ohta H. 2014. Cytoprotective effects of 12-oxo phytodienoic acid, a plant-derived oxylipin jasmonate, on oxidative stress-induced toxicity in human neuroblastoma SH-SY5Y cells. Biochim Biophys Acta 1840:3413–3322.

Taneda S, Honda K, Tomidokoro K, Uto K, Nitta K, Oda H. 2010. Eicosapentaenoic acid restores diabetic tubular injury through regulating oxidative stress and mitochondrial apoptosis. Am J Physiol Renal Physiol 299:F1451–F1461.

Teng FY, Tang BL. 2013. Nogo/RTN4 isoforms and RTN3 expression protect SH-SY5Y cells against multiple death insults. Mol Cell Biochem 384:7–19.

Tokiwa Y, Kitagawa M, Raku T, Yanagitani S, Yoshino K. 2007. Enzymatic synthesis of arbutin undecylenic acid ester and its inhibitory effect on melanin synthesis. Bioorg Med Chem Lett 17:3105–3318.

Van der Steen M, Stevens CV. 2009. Undecylenic acid: A valuable and physiologically active renewable building block from castor oil. ChemSusChem 2:692–713.

Wei JW, Yang LM, Sun SH, Chiang CL. 1987. Phospholipids and fatty acid profile of brain synaptosomal membrane from normotensive and hypertensive rats. Int J Biochem 19:1225–1228.

Yamada T, Hashida K, Takarada-Iemata M, Matsugo S, Hori O. 2011. α-Lipoic acid (LA) enantiomers protect SH-SY5Y cells against glutathione depletion. Neurochem Int 59:1003–1009.

Yin Z, Lee E, Ni M, Jiang H, Milatovic D, Rongzhu L, Farina M, Rocha JB, Aschner M. 2011. Methylmercury-induced alterations in astrocyte functions are attenuated by ebselen. Neurotoxicology 32:291–299.

Yu X, Cui L, Zhang Z, Zhao Q, Li S. 2013. α-Linolenic acid attenuates doxorubicin-induced cardiotoxicity in rats through suppression of oxidative stress and apoptosis. Acta Biochim Biophys Sin (Shanghai) 45:817–826.

Yuste VJ, Sánchez-López I, Solé C, Moubarak RS, Bayascas JR, Dolcet X, Encinas M, Susin SA, Comella JX. 2005. The contribution of apoptosis-inducing factor, caspase-activated DNase, and inhibitor of caspase-activated DNase to the nuclear phenotype and DNA degradation during apoptosis. J Biol Chem 280:35670–35683.

Zhang Z, Larner SF, Liu MC, Zheng W, Hayes RL, Wang KK. 2009. Multiple alphaII-spectrin breakdown products distinguish calpain and caspase dominated necrotic and apoptotic cell death pathways. Apoptosis 14:1289–1298.